metals

MDPI

Article

Strong and Stable Nanocomposites Prepared by High-Pressure Torsion of Cu-Coated Fe Powders

Timo Müller [1,*], Andrea Bachmaier [1], Erich Neubauer [2], Michael Kitzmantel [2] and Reinhard Pippan [1]

1 Erich Schmid Institute of Materials Science, Austrian Academy of Sciences, Leoben 8700, Austria; andrea.bachmaier@oeaw.ac.at (A.B.); reinhard.pippan@oeaw.ac.at (R.P.)
2 RHP-Technology, Seibersdorf 2444, Austria; erich.neubauer@rhp-technology.com (E.N.); michael.kitzmantel@rhp-technology.com (M.K.)
* Correspondence: timo.mueller@oeaw.ac.at; Tel.: +43-3842-804-228

Academic Editor: Chun-Liang Chen
Received: 30 August 2016; Accepted: 19 September 2016; Published: 22 September 2016

Abstract: Segregation and chemical inhomogeneity are well-known problems in powder metallurgy and are also an issue for new applications of powder mixtures, for example as starting materials for severe plastic deformation. In this study, Cu-coated Fe powder was prepared via immersion deposition, inductively hot-pressed and subsequently deformed using high-pressure torsion. The homogeneity of the pressed material was found to be much better than that of powder mixtures that were prepared for comparison. During severe plastic deformation, higher hardness was observed for the coated powder as compared to powder mixtures even after low strains. In the saturation state, the coated powder was found to result in a hardness of about 600 HV, which is significantly harder than for the powder mixtures. This is attributed to the greater amount of impurities introduced by the coating process. It is shown that coated powders are promising starting materials for severe plastic deformation in order to reduce the amount of strain necessary to reach the saturation state and to obtain high strength and more homogeneous mechanical alloying.

Keywords: immersion coating; electroless deposition; severe plastic deformation; high-pressure torsion; nanocomposite

1. Introduction

High-pressure torsion (HPT) is a promising top-down technique to produce bulk nanostructured materials. In contrast to other methods of severe plastic deformation, even very high strains can be obtained easily [1]. Besides HPT deformation of bulk materials, the compaction and deformation of powders has introduced new possibilities to this technique. The oxide film on metal powder particles, for example, results in a higher amount of impurities as compared to bulk material which leads to a smaller saturation grain size and higher hardness during deformation [2]. Also composites of any kind can be obtained easily by mixing the elemental powders of the components [3].

An important issue for severe plastic deformation of composites is the structural homogeneity of the starting material. Although the initial microstructure does not affect the saturation state, which is obtained after a sufficient amount of strain, it has a strong impact on the homogeneity of deformation and the amount of strain which is necessary to obtain this state of saturation [4]. In addition, the structural homogeneity of the starting material is also important for the formation of supersaturated solid solutions. This phenomenon has been reported for many systems, even for systems with a high positive enthalpy of mixing, which are generally considered to be immiscible [5]. Various possible explanations for the supersaturation by plastic deformation have been discussed [6]. Since homogeneous mixtures of small particles provide short diffusion paths, a large amount of

heterogeneous interfaces as well as more parts with very small tips, such a starting material is expected to facilitate intermixing and result in faster formation of supersaturated solutions.

Inhomogeneity can occur in metallurgically prepared starting materials, for example when phase separation occurs on a length scale that approaches the HPT sample size. However, inhomogeneity is also an issue when powder mixtures are used as starting materials. Segregation is especially likely to occur when the various components of the powder mixture differ strongly in size and density, and can be only avoided using laborious techniques of mixing [7]. On the contrary, if one component is added not as a second powder but as a coating on the powder particles of the other component, segregation cannot take place and the two components are separated in an invariable distance depending only on the size of the particle and the thickness of the coating. Coated powders have been used in [2] to deform nickel with a significant amount of oxides homogeneously distributed throughout the sample. However, no HPT deformation of coated powders consisting of two metals has been reported so far, to the authors' knowledge.

Such coated powders are investigated in the present study using the Fe-Cu system. According to the phase diagram, the system can be considered as immiscible, since only negligible intermixing of Fe and Cu occurs at room temperature [8]. However, supersaturated solid solutions have been observed and investigated in many studies using both mechanical alloying (see [9] and references therein) and severe plastic deformation. Investigations on HPT-deformed Fe-Cu alloys have been reported using various starting materials. Teplov et al. [10,11] found single-phase solid solutions of up to 20 at. % Cu on the iron-rich side and up to 20 at. % Fe on the copper-rich side of the phase diagram for both master alloys and powder mixtures as starting materials. Bachmaier et al. [12] developed a two-step HPT process to reduce the saturation grain size and obtain solid solutions in a more efficient way. Up to 15 at. % from both sides of the phase diagram were found to result in single-phase solid solutions [12]. For both alloys from the melt and powder mixtures, a continuous refinement of the Fe particles in Cu-rich alloys via fragmentation and dissolution was reported [13,14]. Also, a composite of iron fibers in a copper matrix has been deformed via HPT and the dissolution of the iron fibers was observed [15–17]. In these studies, an inhomogeneous deformation of the composite due to Fe-rich and Fe-depleted regions in the samples was reported [15,17].

In the present study, copper-coated iron powders as starting materials for HPT deformation were produced via immersion deposition. Immersion deposition is a cheap and versatile technique for coating, since no expensive equipment and no vacuum is required. The immersion deposition of Cu on Fe has been known for more than a century [18]. However, the deposition on powders is more complex since some processing steps (e.g., fast drying) cannot be directly transferred from the plating of macroscopic parts to powders. The coating of Fe powder with Cu via immersion deposition from an electrolyte with citrate complexation was investigated by Turoňová et al. [19]. Citrate complexes slow down the deposition rate [19]. This is not only of interest to reduce the reaction if it is unintended, but also to elongate the deposition process and enable more homogeneous coatings.

The aim of the present study is to investigate the effect of the coated powder on the microstructure and hardness evolution during HPT deformation, as compared to a powder mixture. Special attention is attributed to the homogeneity of the starting material, the deformation behavior as well as the formation of supersaturated solutions.

2. Materials and Methods

In this study, three different configurations of Fe-Cu alloys were deformed via high pressure torsion: a copper-coated iron powder, an undeformed powder mixture of iron and copper powders, and a powder mixture after previous HPT deformation.

The coated powder was produced via immersion deposition. The electrolyte consisted of 0.8 mol·dm^{-3} cupric sulfate pentahydrate and 0.4 mol·dm^{-3} tri-sodium citrate dehydrate. Then 12 g of iron powder (−200 mesh, 99+% purity) were immersed in 0.15 cm^3 of electrolyte for 30 s. During this deposition process the bath was agitated using a magnetic stirrer at 500 rpm. Subsequently,

the powder was removed from the electrolyte using a magnetic rod. It was rinsed with de-ionized water and isopropyl and then dried in a filter paper (grade MN 615). This procedure was repeated various times to obtain larger amounts of coated powders. Using only small amounts of powders at once enabled the fast removal of the powder from the electrolyte as well as homogeneous coating. The coated powder was compacted by RHP-Technology (Seibersdorf, Austria) using inductive hot pressing at 650 °C and 30 MPa for 15 min. Subsequently, disks of 8 mm diameter and about 0.8 mm height were cut out of the compacted composite and used for HPT deformation.

For comparison, a powder mixture was prepared consisting of 16 g (33 wt. %) copper powder (−70 + 400 mesh, 99.9% purity) and 32 g (67 wt. %) iron powder (−100 + 200 mesh, 99.9% purity). It was compacted and cut in the same way as described above for the coated powder.

Besides, a mixture of iron and copper powder, which had been pre-deformed in a larger HPT device, was also used for comparison. A mixture of Fe70Cu30 was prepared from copper (−170 + 400 mesh, 99.9% purity) and iron (−100 + 200 mesh, 99.9% purity) powders. The powder mixture was compacted and a disk of 50 mm diameter and 9.5 mm thickness was deformed via HPT (10 rotations). Disks with 8 mm diameter and about 0.8 mm thickness were cut in such a way from the larger HPT disk, that the axial direction for the following deformation experiments was approximately the radial direction of the previous deformation. A detailed description of this two-step HPT process can be found in [12].

All samples were deformed via HPT at a pressure of 7.3 GPa with a sample size of 8 mm diameter and about 0.8 mm height. For deformation at elevated temperatures, the anvils and the sample were heated inductively. Room temperature experiments were performed at 0.2 rpm, whereas at elevated temperatures 0.6 rpm was used to reduce deformation time.

The structure of the undeformed and deformed state was investigated using light microscopy as well as scanning electron microscopy (SEM LEO 1525 from Zeiss, Oberkochen, Germany) with a back-scattered electron detector and an electron backscatter diffraction (EBSD) system from EDAX, Mahwah, NJ, USA. Grain size distributions of undeformed materials were obtained directly from EBSD measurements, whereas the grain size after deformation was estimated from manual analysis of SEM images obtained with the back scattered electron detector using ImageJ software. The given grain sizes are the shorter axis of fitted ellipses. The composition of the samples was also investigated with this device using an energy-dispersive x-ray spectroscopy (EDX) system from Oxford Instruments, Abingdon, UK. Vickers microhardness was measured using a Micromet 5104 (from BUEHLER, Chicago, IL, USA) with a load of 100 g (HV 0.1). All microstructural investigations and hardness measurements were carried out on a central cross-section of the HPT disc in tangential direction at different radii.

X-ray diffraction (XRD) experiments were performed with a SmartLab diffractometer (Rigaku Europe SE, Ettlingen, Germany) in parallel beam geometry using Cu-Kα radiation and a secondary monochromator in Leoben. Half of an HPT specimen with the axial direction parallel to the diffraction vector was used for these measurements. For analysis of peak position and peak width, the XRD pattern were fitted with pseudo-Voigt profiles and a parabolic background using Fityk software [20].

3. Results

3.1. Initial Structure of the Coated Powder

The as-coated powder consists of Fe cores coated with a Cu layer of about 1–2 µm thickness. The size of the Fe cores varies from a few micrometers up to about a hundred micrometers in the long axis of the mostly ellipsoidal particles. As shown in Figure 1a, the Cu layer does not stick directly on the Fe. This poor adhesion might explain the Cu shells without cores that have been observed in the cross-sections of as-coated powder (Figure 1a), since the Fe core might have been removed during cross-section preparation. Besides, some small pure Cu particles with a size of a few microns are observed in the powder after coating. These might originate either from small Fe powder particles, which were replaced by Cu completely in the deposition process, or from larger Cu shells, which broke

due to collisions of particles during powder processing. An improvement of the adhesion and quality of the coating might be achieved using a smaller particle concentration in the electrolyte [19]. However, this is not investigated in the present study, since good adhesion is not absolutely necessary for the further processing and the amount of electrolyte to produce the same amount of powder would significantly increase.

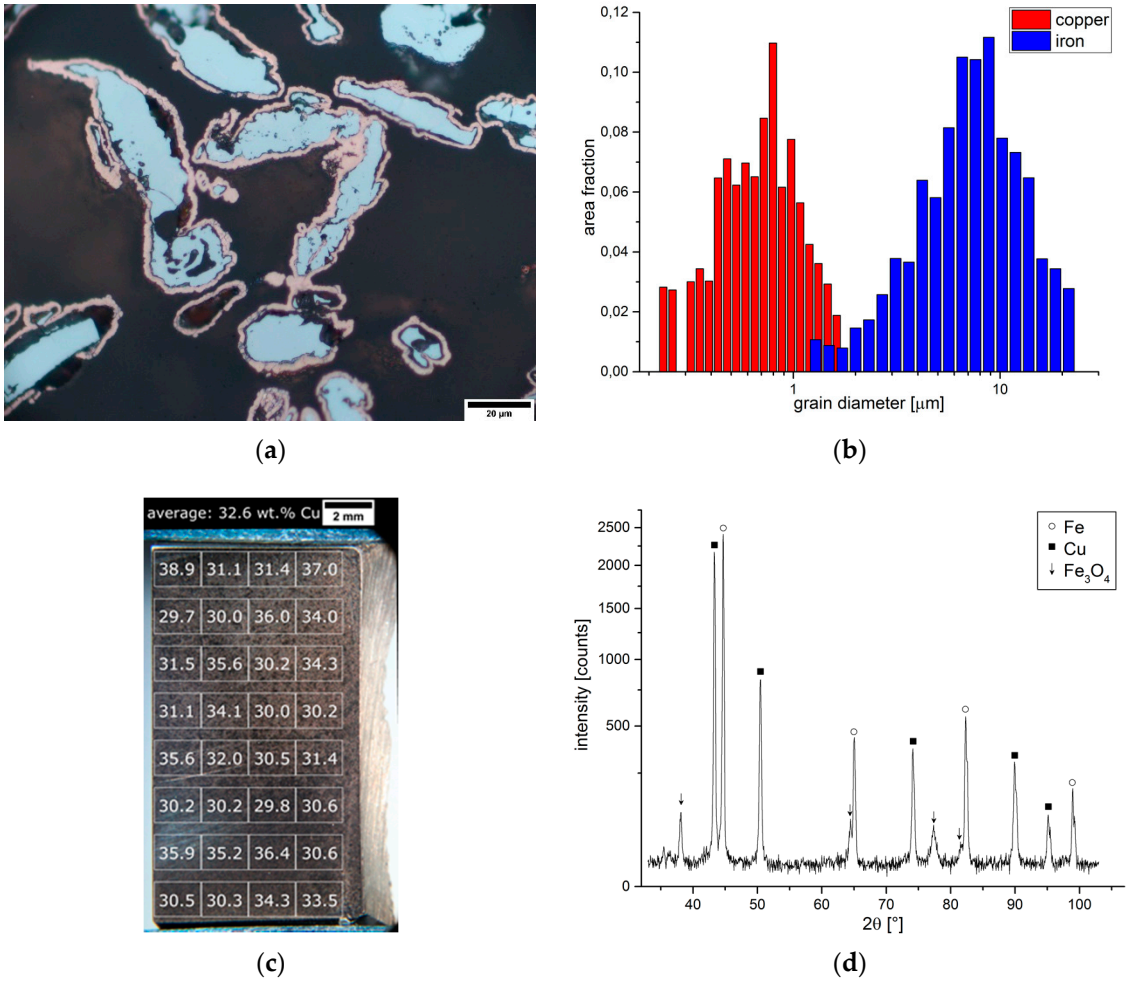

Figure 1. Structure of the coated powder before deformation: (**a**) Optical micrograph of a cross-section of powder particles after coating; (**b**) Grain size distributions of Cu and Fe phases after hot pressing as obtained from EBSD measurements; (**c**) Light micrograph of a cross-section of the hot-pressed coated powder. The white overlay indicates the EDX measurement areas and the numbers give the measured Cu contents in wt. %; (**d**) XRD pattern after hot pressing indicates a three-phase mixture of Fe, Cu and magnetite.

After inductive hot pressing, the Fe cores of the coated powder particles are still apparent in the microstructure and are separated by a Cu layer network. Most grains of the Cu phase are in the ultra-fine grained region, whereas the Fe grains are 10 times larger (Figure 1b). On a length scale up to tens of microns, Fe- and Cu-rich regions can be found due to the size of the original powder particles. However, the material is very homogeneous on a larger scale (Figure 1c). The overall composition as determined via EDX is 33 wt. % Cu and 67 wt. % Fe.

XRD measurements (Figure 1d) show the presence of magnetite, Fe_3O_4, in the coated powder. A magnetite content of about 5 wt. % was determined using TOPAS software [21].

3.2. Initial Structure and Homogeneity of the Powder Mixtures

The powder mixture, which was also inductively hot-pressed, is very inhomogeneous on a macroscopic scale. Figure 2a shows the results of EDX measurements on a cross-section of the hot-pressed material. The concentrations scatter over a larger range on a length scale that is comparable to the size of the HPT samples. Besides the chemical inhomogeneity, a quite coarse structure is observed (Figure 2b). The individual Cu and Fe particles in the pressed material have a size up to several hundred microns. This is a consequence of particle clusters since the original powder particles were significantly smaller.

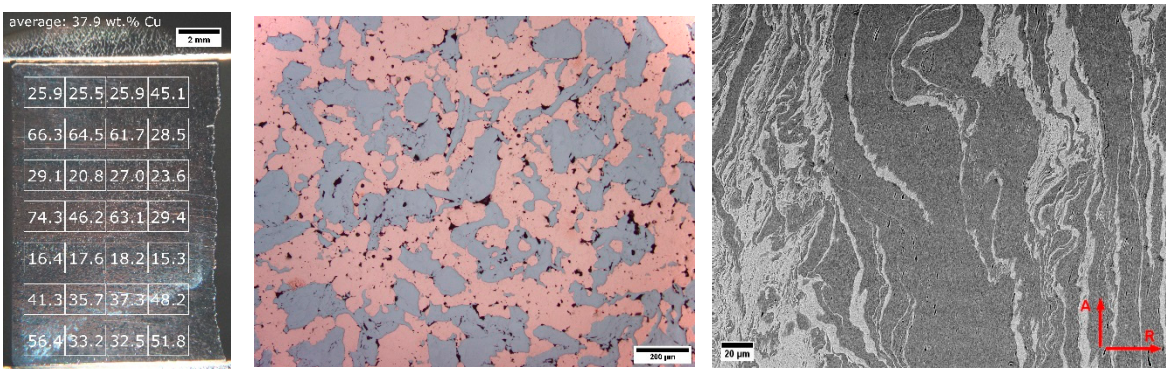

(**a**) (**b**) (**c**)

Figure 2. Structure of the powder mixtures before deformation: (**a**) Optical micrograph of a cross-section of the hot-pressed powder mixture. The numbers in the overlay give the Cu contents in wt. % as obtained from EDX with measuring regions indicated by the white grid; (**b**) Optical micrograph showing the coarse structure of the hot-pressed powder mixture (in a Cu-rich region); (**c**) Back-scattered electron micrograph of the pre-deformed powder mixture. The arrows indicate the axial (A) and radial (R) directions of the second HPT step.

The second powder mixture, which was already pre-deformed in a large HPT tool, shows the typical structure of elongated particles after the first deformation step (Figure 2c). The Cu grains are almost spherical with a grain size of about 200 nm, whereas the Fe grains are mostly elongated with a grain size of 200 to 1000 nm in the long axis and 50 to 300 nm in the short axis. The samples for the second HPT deformation step are cut in such a way that the elongated grains are oriented with the long axis almost parallel to the axial direction of the second HPT deformation (Figure 2c). This results in a re-orientation of the grains in the second deformation step which is expected to accelerate the refinement process. For both powder mixtures, a two-phase mixture of Fe and Cu without any indication of oxides is revealed by XRD.

3.3. Structures and Hardness Evolution during Deformation at Room Temperature

For an HPT deformation of up to two turns, the structure refinement results in a linear increase of hardness with applied equivalent strain. The same hardening rate is observed for both the coated powder and the two-step HPT material (Figure 3a). Also the hardness in the center of the HPT discs, where no strain is applied in the idealized case, is the same for these two starting materials. This can be attributed to the ultra-fine-grained structure, which is present in the two-step HPT samples due to the previous deformation and in the Cu phase of the coated powder due to the coating process.

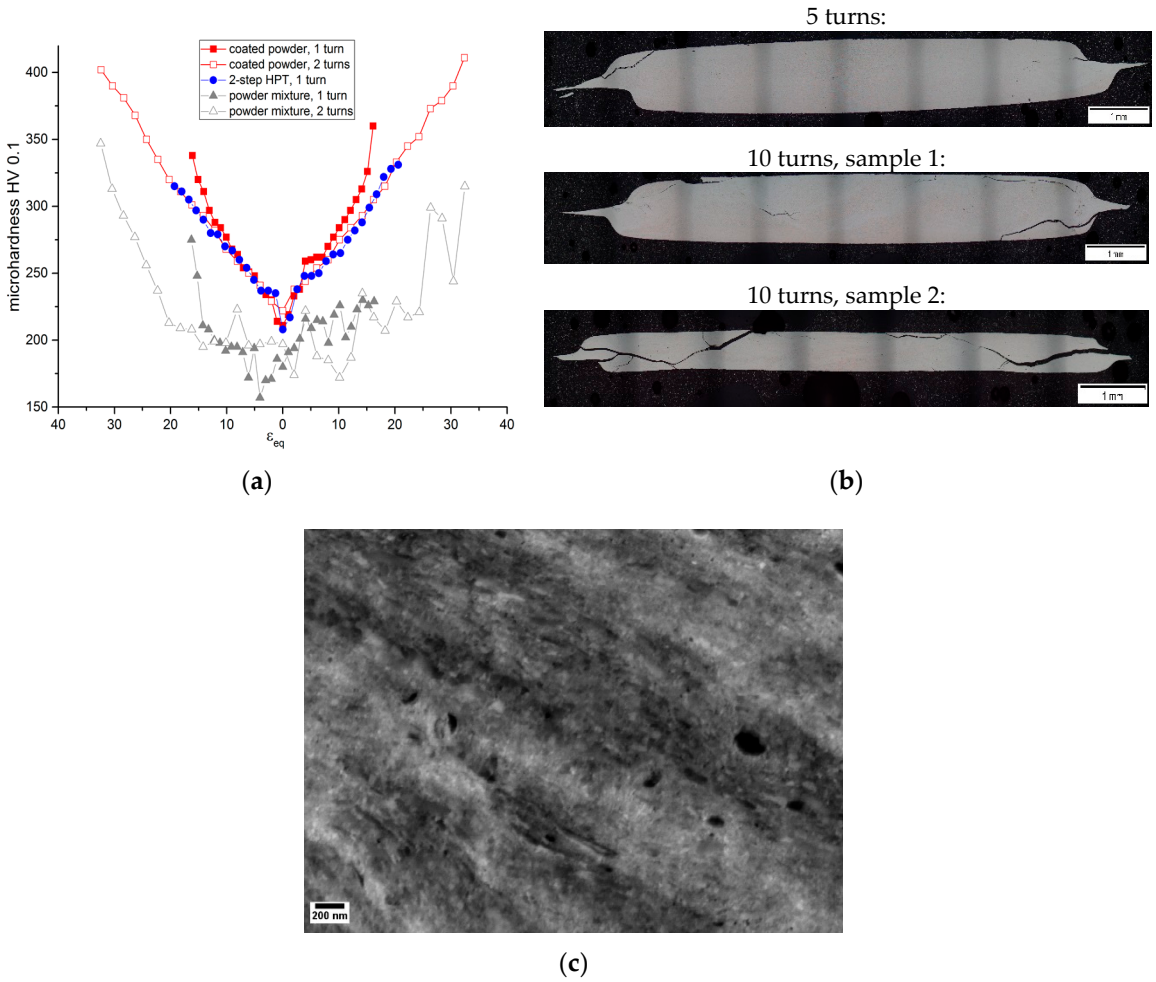

Figure 3. Structure and hardness evolution during HPT at room temperature: (**a**) Hardness profiles after one and two turns; (**b**) Optical micrographs of coated powder samples deformed by five or 10 turns, respectively; (**c**) Microstructure of a coated powder sample after 50 rotations at a radius of 3 mm (ε_{eq} = 700) imaged with back-scattered electron detector.

On the contrary, the hardness of the powder mixture samples is lower and a larger scatter occurs over the cross-section of an HPT sample (Figure 3a). The lower hardness is due to the coarser microstructure in the initial state. The scatter originates from both the chemical inhomogeneity and from the fact that the size of the Cu and Fe phase regions is of the same size or even larger than the microhardness indents. Hence, a higher or lower hardness is measured depending if the indent is placed in a Fe- or Cu-rich region, respectively. Nonetheless, the hardness of the powder mixture increases at approximately the same rate as the other two materials.

Whereas the powder mixtures with and without previous deformation are deformable up to extremely high strains (ε_{eq} > 1000), an increasing probability of crack formation with increasing strain is observed for the coated powder. After five turns (corresponds to ε_{eq} = 90 at the edge of the HPT disk), the first cracks occur at the edge of the sample. With further deformation, the number of cracks significantly increases (Figure 3b). We assume that these cracks are formed during unloading after deformation. Therefore, the hardness profiles were also measured for fractured samples, since the structure evolution during deformation and thus the hardness should not be influenced. Such materials are of no practical use, and a way to avoid the formation of cracks will be discussed in the next paragraph.

After 50 turns, the hardness starts to saturate at the sample edge for all three starting materials (Figure 4b). Whereas with the coated powder a hardness of about 600 HV is obtained, both powder mixtures reach a maximum hardness of about 450 to 500 HV. For all three materials a nanocrystalline microstructure is obtained, which consists of regions of equi-axed grains co-existing with regions of elongated grains with the short axis in the axial direction of the HPT process (Figure 3c). Cu- and Fe-rich regions can no longer be distinguished in the SEM images for all three starting materials. The grain size in the coated powder sample is about 30 nm, whereas for the two-step HPT sample the grain size ranges from 50 to 100 nm. For the one-step HPT powder mixture, most parts of the sample are similar to the two-step HPT material. However, ultra-fine-grained regions with grain sizes up to several hundred nanometers are also observed, even at the edge of the sample after 50 turns (ε_{eq} = 900).

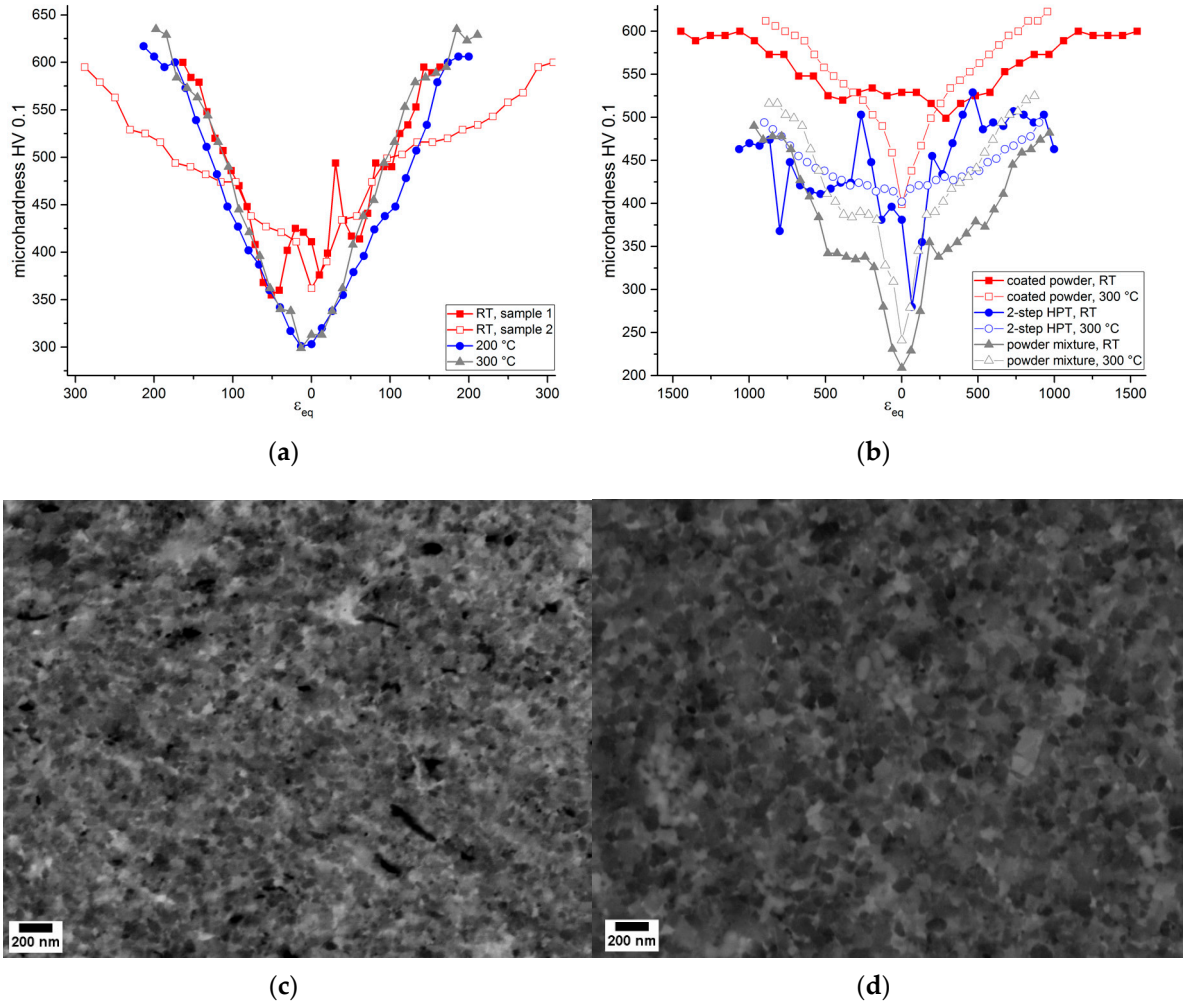

Figure 4. The effect of elevated temperature on the structure and hardness evolution: (**a**) Hardness profiles of HPT samples from coated powder after 10 turns at different temperatures (the differences between the two room-temperature samples can be attributed to different amounts of cracking, cf. Figure 3b); (**b**) Hardness profiles of HPT samples after 50 turns; Back-scattered electron micrographs of (**c**) coated powder and (**d**) pre-deformed (two-step HPT) powder mixture after 50 turns at 300 °C, measured at a radius of 3 mm (ε_{eq} = 700 without previous deformation).

In the XRD patterns, all peaks of Fe and Cu are broadened and shifted towards smaller diffraction angles with an increasing amount of strain (Figure 5). A correlation of the broadening and the peak shift is observed. After 50 turns both the peak widths and the peak shifts are significantly larger for the

coated powder sample as compared to the powder mixtures. The broadening and peak shifts of the two powder mixtures are very similar, with a tendency of slightly more broadening and peak shift for the two-step HPT sample. These results fit in well with the smaller grain size observed for the coated powder sample. However, no quantitative analysis of grain size or lattice parameters from the XRD data is performed, since strong nonlinearities are observed in the Williamson-Hall and Nelson-Riley plots, respectively. Possible explanations will be discussed in Section 4.3. For all deformed samples, no indications of oxide phases are found.

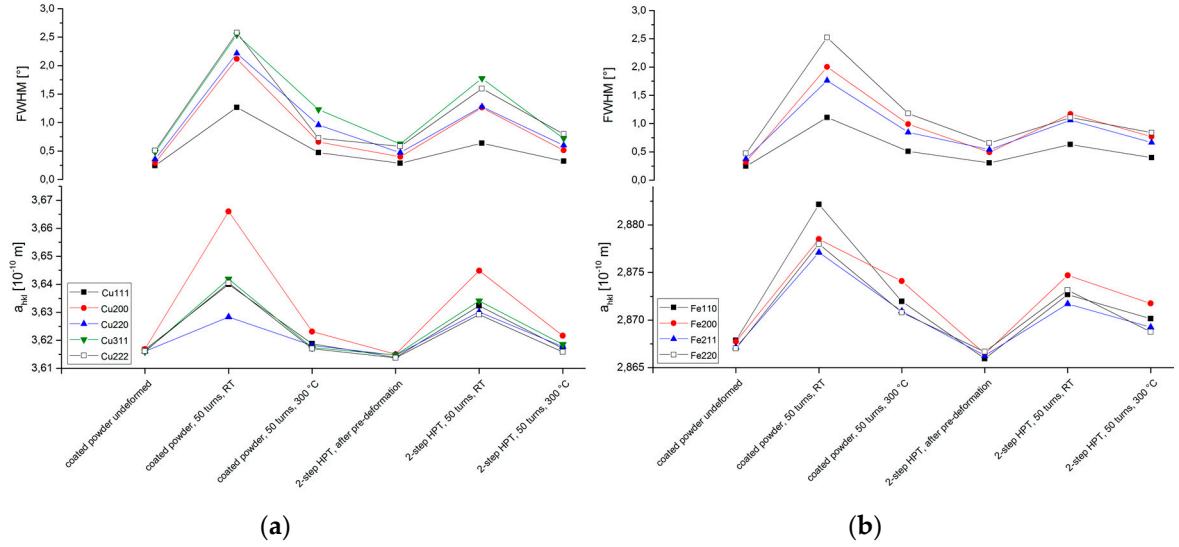

Figure 5. Peak width (full width at half maximum, FWHM) and lattice parameter calculated from the XRD peak positions, a_{hkl}, for the (**a**) Cu and (**b**) Fe phases.

3.4. Structures and Hardness Evolution during Deformation at Elevated Temperatures

To avoid the formation of cracks in the HPT samples of the coated powder, the deformation was performed at elevated temperatures. For all samples deformed at 300 °C, no severe cracking occurred. Figure 4a shows the hardness profiles of coated powder samples after 10 turns of HPT deformation at different temperatures. The same hardness evolution is obtained independent of the deformation temperature. For the deformation at room temperature, a slightly higher hardness is obtained near the center of the HPT disc. However, this is not caused by the deformation temperature, but might be due to a larger misalignment of the central axis of the HPT tool in these experiments.

Also, the saturation hardness, which is obtained after 50 turns at the edge of the sample (ε_{eq} = 900), is similar to the room temperature experiments for all three starting materials (Figure 4b). The difference in hardness of the coated powder sample as compared to the powder mixtures corresponds to a difference in grain size. For the coated powder, the grain size in saturation is about 30 to 50 nm (Figure 4c), whereas for the powder mixtures 60 to 100 nm are measured for both the one-step and two-step HPT deformation (Figure 4d). In contrast to the microstructures after deformation at room temperature, no regions with elongated grains are observed in the saturated regions of the samples deformed at elevated temperatures. As for samples deformed at room temperature, Cu- and Fe-rich regions cannot be distinguished in the SEM images of the saturated state anymore. Hence, only average grain sizes can be given.

XRD peak broadening and peak shifts towards smaller diffraction angles also occur for all samples deformed at 300 °C. As for the room temperature experiments, the broadening and the peak shifts are larger for the coated powder sample than for the powder mixtures (Figure 5). For the latter, no differences of one-step and two-step samples are observed. However, the broadening and the peak shifts obtained after deformation at 300 °C are significantly smaller than for deformation at room

temperature. The peak widths and shifts of the coated powder sample deformed at 300 °C are similar to those of the powder mixtures deformed at room temperature for the Fe phase; for the Cu phase they are even smaller. The smaller broadening as compared to the room temperature samples cannot be attributed to a smaller grain size, since the grain size measured in SEM is the same. However, smaller densities of dislocations and small angle boundaries [22] due to dynamic recovery processes during HPT at elevated temperature may explain the smaller peak broadening. Interestingly, a similar hardness is obtained in spite of these differences in structure.

4. Discussion

It has been shown that materials with higher saturation hardness can be obtained from HPT deformation of Cu-coated Fe powder as compared to powder mixtures of Fe and Cu. While the coated starting powders are prone to cracking when deformed at room temperature, extremely high strains can be applied without fracture at elevated temperature. In the following, the impact of the two main differences of the starting materials, chemical homogeneity and impurity concentration, on the structure evolution as well as the resulting differences concerning intermixing of Cu and Fe during deformation will be discussed.

4.1. Homogeneity of the Materials

The chemical inhomogeneity of the powder mixture after hot pressing (Figure 2a) results in HPT samples in which the composition varies to a significant extent, both from one sample to another as well as within each sample. The former will result in a scatter of evolving structures and properties. Since the Cu phase is generally softer than the Fe phase, samples with a higher Cu content result in a lower overall hardness after deformation. The inhomogeneity within one sample results in inhomogeneous deformation, strain concentrations and non-symmetric hardness profiles as shown in Figure 3a.

On the very contrary, the coated powder results in very homogeneous structures on all length scales larger than the size of the original powder particles. For all HPT samples from the coated powder, the Cu concentration from EDX measurements varied by less than 6 wt. %. This homogeneity results in a more uniform deformation and stronger work hardening in the HPT process and consequently in a lower scatter of the hardness profiles (Figures 3a and 4a,b). This makes the structure and the properties of the material after deformation more predictable and therefore more suitable for possible applications. The stronger work hardening is assumed to be due to the higher concentration of heterogeneous interfaces in the initial structure, providing obstacles for dislocation movement, as well as the enhanced intermixing (cf. Section 4.3) impeding the motion of dislocation via pinning of substitutional elements. In addition, the size restriction of Cu- and Fe-rich regions to the size of the initial powder particles reduces the distance of material transport, which has to be achieved via plastic flow to obtain a completely homogeneous saturation state after a certain amount of strain. Therefore, the state of saturation is reached faster than for starting materials where chemical inhomogeneity on a larger length scales is present.

Concerning homogeneity, the pre-deformed powder mixture lies between the undeformed powder mixture and the coated powder. Cu- and Fe-rich regions on a length scale of several hundred micrometers are observed. Nevertheless, quite symmetric hardness profiles are obtained even at low strains of the second HPT deformation step (Figure 3a). This is attributed to the preliminary HPT deformation step. The change of the rotation axis from the first to the second HPT step results in an alignment of the lamellar structure after the first step that accelerates further structure refinement in the second step [12]. Therefore, the same hardness values as for the coated powder can be obtained at low strains (Figure 3a). Since the structure and the properties in the saturation state are known not to depend on the microstructure of the starting material [4], the differences of powder mixtures and coated powder at larger strains cannot be a result of the differences in homogeneity and possible explanations for the differences in the saturation state will be discussed in the following.

4.2. The Role of Impurities

As revealed from XRD, the coated powder contains a significant amount of oxides. The bad adhesion of the Cu coating and the compact nature of the Fe cores indicate that the Fe powder particles are oxidized at the surface when immersed in the electrolyte. Since Fe forms no dense oxide films, the coating process is not severely impeded by this oxide film. Also the powder mixtures contain some oxides, since it is well known that both Cu and Fe form native oxide films on their surfaces and the specific surface of the powders is relatively high [23]. However, the oxide content in the powder mixtures is significantly lower than for the coated powder, which is evident from the XRD patterns.

The oxides found in the coated powder samples represent hard inclusions in a softer metallic matrix. During deformation, fragmentation occurs and parts of the oxides may dissolve in the matrix. Nevertheless, the oxides cause embrittlement and cracking of the samples for room temperature deformation. At elevated temperatures, stress concentrations caused by the oxide particles are reduced due to dynamic recovery and rewelding of small microcracks is more likely to occur. Therefore, no cracks are observed for coated powder samples deformed at elevated temperatures.

Besides this impact on the deformability of the material, the higher amount of oxides in the coated powder also affects the structure and properties in the saturation state. It is well known that the saturation state is a steady state determined by the competition of grain refinement via plastic deformation on the one hand, and dynamic recovery, thermally or mechanically induced coarsening, on the other hand [1]. No oxide peaks are observed in XRD after deformation. Either the size of the oxides is reduced during deformation to such an extent that the broadened Bragg peaks of the oxide vanish in the background and the neighboring peaks of the metal phases, or parts of the oxygen dissolve in the matrix. Both atomic oxygen and oxide particles on the nanometer scale provide obstacles for the movement of grain boundaries and stabilize a finer microstructure. The thermal stability of the nanocrystalline microstructure at 300 °C can also be attributed to the stabilization of the grain boundaries by the impurities, which may be thermodynamically or kinetically driven [24].

In this context, the enhanced impurity level in the coated powder might be a further advantage of these materials as starting materials for HPT deformation, since stronger materials can be obtained, which are also thermally stable up to a certain temperature. However, these effects might also be achieved via powder mixtures with enhanced impurity content. To separate the effects of homogeneity and contamination on the structure and hardness evolution at low strains, further studies with coated powders of different contamination levels, which may be obtained via different coating processes, would be necessary. Nevertheless, the effects of more homogeneous deformation and less strain to obtain the saturation state (as discussed in Section 4.1) are assumed to be mainly due to the homogeneity of the powder mixture and not the higher amount of impurities. These effects could therefore not be obtained with powder mixtures of higher-impurity contents.

4.3. Mechanical Alloying

The shifts of the Bragg peaks of both fcc and bcc phases towards lower diffraction angles indicate mechanical alloying of Cu and Fe. However, macroscopic residual stresses and, for the Cu phase, the formation of stacking faults may result in additional peak shifts. Also a dependence of the lattice parameter, i.e., the shift of Bragg peaks, as a function of grain size has been discussed in the literature [25]. However, the same peak shifts, which were observed in the present study, have already been described by Bachmaier et al. [12] for the two-step HPT process of Fe-Cu alloys with different compositions, for which supersaturated solid solutions were also observed. In addition, the increase of the lattice parameter with the increasing solute concentration on both sides of the Fe-Cu phase diagram has been reported for supersaturated solid solutions by quenching [26] and ball milling [27]. Therefore, it can be concluded that the mutual intermixing of Fe and Cu is the main reason for the observed peak shifts.

With this assumption, the XRD results show an increasing amount of mechanical alloying with increasing peak broadening, i.e., decreasing grain size and increasing microstrain or increasing

dislocation density. The larger peak shifts for the deformed coated powder as compared to the powder mixtures indicate that a larger amount of Fe is dissolved in the Cu phase, and vice versa, for the coated powder as starting material. Possible reasons are the smaller grain size and higher densities of stored dislocations, which are both stabilized by the higher amount of impurities. Therefore, the coated powder as a starting material seems to promote the mechanical alloying. However, more detailed investigations are necessary to manifest this assumption, since also the dissolution of interstitials (e.g., oxygen) from the impurities itself may result in an increase of the lattice parameter, i.e., in a peak shift towards lower angles.

5. Conclusions

It is shown that coated powders are an appropriate alternative to powder mixtures in order to improve both the initial structural homogeneity and the homogeneity of deformation in HPT samples prepared via the powder route. The higher homogeneity enables obtaining harder materials even with low strains. Besides, modifications of the material due to the coating process change the structure and properties in the saturation state of severe plastic deformation. In this study, an enhanced impurity concentration induced by immersion coating results in higher hardness due to the impeded grain boundary motion which impedes grain growth and shifts the equilibrium between grain refinement and dynamic recovery towards a smaller grain size.

Acknowledgments: Funding for this work has been provided by the Austrian Science fund (FWF): J3468-N20 and the European Research Council under ERC Grand Agreement No. 340185 USMS.

Author Contributions: T.M., A.B., and R.P. conceived and designed the experiments. T.M. performed the experiments and wrote the manuscript. E.N. and M.K. mixed and compacted the powders. A.B. prepared the pre-deformed HPT material. All authors contributed to the finalization of the manuscript.

Conflicts of Interest: The authors declare no conflict of interest.

References

1. Pippan, R.; Wetscher, F.; Hafok, M.; Vorhauer, A.; Sabirov, I. The Limits of Refinement by Severe Plastic Deformation. *Adv. Eng. Mater.* **2006**, *8*, 1046–1056. [CrossRef]
2. Bachmaier, A.; Hohenwarter, A.; Pippan, R. New Procedure to Generate Stable Nanocrystallites by Severe Plastic Deformation. *Scr. Mater.* **2009**, *61*, 1016–1019. [CrossRef]
3. Bachmaier, A.; Pippan, R. Generation of metallic nanocomposites by severe plastic deformation. *Int. Mater. Rev.* **2013**, *58*, 41–62. [CrossRef]
4. Pippan, R.; Bachmaier, A.; Hohenwarter, A.; Renk, O. Nanocomposites and super saturated solid solutions generated by SPD: The effect of initial structure and strain path. In *Nanometals-Status and Perspective*, Proceedings of the 33rd Risø International Symposium on Materials Science, Roskilde, Denmark, 3–7 September 2012; Faester, S., Ed.; Department of Wind Energy, Technical University of Denmark: Roskilde, Denmark, 2012; pp. 107–113.
5. Suryanarayana, C. Mechanical alloying and milling. *Prog. Mater. Sci.* **2001**, *46*, 1–184. [CrossRef]
6. Raabe, D.; Choi, P.-P.; Li, Y.; Kostka, A.; Sauvage, X.; Lecouturier, F.; Hini, K.; Kirchheim, R.; Pippan, R.; Embury, D. Metallic Composites Processed via Extreme Deformation: Toward the Limits of Strength in Bulk Materials. *MRS Bull.* **2010**, *35*, 982–991. [CrossRef]
7. Thümmler, F.; Oberacker, R. *Introduction to Powder Metallurgy*; The Institute of Materials Series on Powder Metallurgy: London, England, 1993; p. 113.
8. Predel, B. Cu-Fe (Copper-Iron). In *Landolt-Börnstein–Group IV: Physical Chemistry (Cr-Cs–Cu-Zr)*; Madelung, O., Ed.; Springer: Berlin, Germany, 1994; Volume 5D. [CrossRef]
9. Jiang, J.Z.; Gente, C.; Bormann, R. Mechanical Alloying in the Fe-Cu System. *Mater. Sci. Eng.* **1998**, *A242*, 268–277. [CrossRef]
10. Teplov, V.A.; Pilugin, V.P.; Gaviko, V.S.; Chernyshov, E.G. Non-equilibrium Solid Solution and Nanocrystal Structure of Fe-Cu Alloy after Plastic Deformation under Pressure. *Phil. Mag. B* **1993**, *68*, 877–881. [CrossRef]

11. Teplov, V.A.; Pilugin, V.P.; Gaviko, V.S.; Chernyshov, E.G. Nanocrystalline Structure of Non-equilibrium Fe-Cu Alloys Obtained by Severe Plastic Deformation under Pressure. *Nanostr. Mater.* **1995**, *6*, 437–440. [CrossRef]
12. Bachmaier, A.; Kerber, M.; Setman, D.; Pippan, R. The Formation of Supersaturated Solid Solutions in Fe-Cu Alloys Deformed by High-Pressure Torsion. *Acta Mater.* **2012**, *60*, 860–871. [CrossRef] [PubMed]
13. Lukyanov, A.; Churakova, A.; Filatov, A.; Levion, E.; Valiev, R.; Gunderov, D.; Antipov, E. Microstructure Refinement in Cu-Fe Alloys Using High Pressure Torsion. *IOP Conf. Ser. Mater. Sci. Eng.* **2014**, *63*, 012102. [CrossRef]
14. Krämer, L.; Wurster, S.; Pippan, R. Deformation Behavior of Cu-Composites Processed by HPT. *IOP Conf. Ser. Mater. Sci. Eng.* **2014**, *63*, 012026. [CrossRef]
15. Sauvage, X.; Wetscher, F.; Pareige, P. Mechanical Alloying of Cu and Fe Induced by Severe Plastic Deformation of a Cu-Fe composite. *Acta Mater.* **2005**, *53*, 2127–2135. [CrossRef]
16. Sauvage, X.; Pippan, R. Nanoscaled Structure of a Cu-Fe Composite Processed by High-Pressure Torsion. *Mater. Sci. Eng. A* **2005**, *410–411*, 345–347. [CrossRef]
17. Quelennec, X.; Menand, A.; le Breton, J.M.; Pippan, R.; Sauvage, X. Homogeneous Cu-Fe Supersaturated Solid Solutions Prepared by Severe Plastic Deformation. *Phil. Mag.* **2010**, *90*, 1179–1195. [CrossRef]
18. Clark, W.G. Improved Method of Coating Thin Iron or Steel Sheets, Wire or Tubing, or Small Iron Articles such as Nails or Screws, with Copper or its Alloys. Patent GB 13445, 1909.
19. Turoňová, A.; Gálová, M.; Gernátová, M. Study of Electroless Copper Deposition on Fe Powder. *Particul. Sci. Technol.* **2008**, *26*, 126–135. [CrossRef]
20. Wojdyr, M. Fityk: A general-purpose peak fitting program. *J. Appl. Cryst.* **2010**, *43*, 1126–1128. [CrossRef]
21. TOPAS V4: General profile and structure analysis software for powder diffraction data. User's manual; Bruker AXS: Karlsruhe, Germany, 2008. Available online: http://algol.fis.uc.pt/jap/TOPAS%204-2%20Users%20Manual.pdf (accessed on 20 September 2016).
22. Ungár, T.; Tichy, G.; Gubicza, J.; Hellmig, R.J. Correlation between subgrains and coherently scattering domains. *Powder Diffr.* **2005**, *20*, 366–375.
23. Suzuki, S.; Ishikawa, Y.; Isshiki, M.; Waseda, Y. Native oxide layers formed on the surface of ultra high-purity iron and copper investigated by angle resolved XPS. *Mater. Trans. JIM* **1997**, *38*, 1004–1009. [CrossRef]
24. Andrievski, R.A. Review of thermal stability of nanomaterials. *J. Mater. Sci.* **2014**, *49*, 1449–1460. [CrossRef]
25. Rane, G.K.; Welzel, U.; Meka, S.R.; Mittemeijer, E.J. Non-monotonic lattice parameter variation with crystallite size in nanocrystalline solids. *Acta Mater.* **2013**, *61*, 4524–4533. [CrossRef]
26. Klement, W. Solid solutions in copper-iron alloys quenched rapidly from the melt. *Trans. Met. Soc. AIME* **1965**, *233*, 1080–1082.
27. Gaffet, E.; Harmelin, M.; Faudot, F. Far-from equilibrium phase transition induced by mechanical alloysing in the Cu-Fe system. *J. Alloy. Comd.* **1993**, *194*, 23–30. [CrossRef]